

---

# Variational inference of latent state sequences using Recurrent Networks

---

**Justin Bayer**

Lehrstuhl für Echtzeitsysteme und Robotik  
Fakultät für Informatik  
Technische Universität München  
bayer.justin@googlemail.com

**Christian Osendorfer**

Lehrstuhl für Echtzeitsysteme und Robotik  
Fakultät für Informatik  
Technische Universität München  
osendorf@in.tum.de

## Abstract

Recent advances in the estimation of deep directed graphical models and recurrent networks let us contribute to the removal of a blind spot in the area of probabilistic modelling of time series. The proposed methods i) can infer distributed latent state-space trajectories with nonlinear transitions, ii) scale to large data sets thanks to the use of a stochastic objective and fast, approximate inference, iii) enable the design of rich emission models which iv) will naturally lead to structured outputs. Two different paths of introducing latent state sequences are pursued, leading to the variational recurrent auto encoder (VRAE) and the variational one step predictor (VOSP). The use of independent Wiener processes as priors on the latent state sequence is a viable compromise between efficient computation of the Kullback-Leibler divergence from the variational approximation of the posterior and maintaining a reasonable belief in the dynamics. We verify our methods empirically, obtaining results close or superior to the state of the art. We also show qualitative results for denoising and missing value imputation.

## 1 Introduction

Probabilistic modelling enables a wide range of tasks which are of central interest in data processing, with outlier detection, synthesis, missing value imputation and denoising being the most relevant. The data generating distribution of sequences  $\mathbf{x}_{1:T} \in \mathcal{S}^*$  over some space  $\mathcal{S}$  is usually modelled as a product over the individual time steps<sup>1</sup>, i.e.

$$p(\mathbf{x}_{1:T}) = \prod_{t=1}^T p(x_t | \mathbf{x}_{1:t-1}), \quad (1)$$

where the individual factors on the right hand side are represented by an adequate model.

In the simplest cases, the individual factors of Equation (1) are factorised Bernoulli or Gaussian distributions. While still being a reasonable approximation in many cases, treating the different components of each  $x_t$  as independent in such a way is an invalid assumption in many fields. Domains such as vision, audio and robotics notoriously feature problems with complex relations between the observed variables.

This can be overcome as distributions of arbitrary complexity can be chosen for each  $x_t$ . As long as it can be parametrised by a finite set of sufficient statistics, the outputs of some model can be identified with these statistics to represent the distribution of interest. The most common example along these lines is that of mixture density outputs [5] which have also been used with recurrent neural networks (RNNs) for sequential data in general [25] and in the context of probabilistic modelling [9]. This

---

<sup>1</sup>We define  $\mathbf{x}_{1:0} := \emptyset$ .

approach comes at a cost, which is the additional parameters necessary. In the most extreme case, that of a mixture of multivariate Gaussians with full covariance matrices, it grows quadratically in the number of output dimensions.

Arguably the use of distributions for  $x_t$  which have many different maxima and allow higher-order correlations in the individual components is promising. A novel approach using continuous latent variables, stochastic gradient variational Bayes (SGVB), has been put forward independently by [17] and [23] to represent complex, nonlinear dependencies between distinct components of the observed variables for the static case. As opposed to many competing approaches, such as deep belief networks [15] and generative stochastic networks [4], a proper objective function, obtaining independent samples and efficient estimation of the marginal likelihood is possible.

We will apply SGVB to two different introductions of latent variables in  $p(\mathbf{x}_{1:T})$  making use of RNNs as the building blocks. Our method retains many of the useful properties of neural networks. Their discriminative nature makes it possible to model rich distributions, i.e. those which are parametrizable by a finite set of statistics (e.g. the exponential family) and mixtures thereof. We can rely on a broad range of optimisation and regularisation methods. Additionally, neural networks have shown to be applicable to a wide range of data. Another central contribution is that of using Wiener processes as priors for the latent states, which represent a good trade-off between expressiveness and tractability.

## 1.1 Related Work

Recurrent neural networks have regained interest recently, achieving competitive results in the areas of natural language processing [9, 18], speech recognition [11] and handwriting recognition [10]. Simultaneously, the theoretical efforts have lead to a better understanding of the learning dynamics [21] and the options of making RNNs more powerful have improved by means of architecture, learning and regularization [20, 13, 1, 3, 6]. A practical variational approach for RNNs has been described by [8], albeit it focuses on variational learning of the parameters.

Using RNNs for probabilistic time series modelling is often done with a combination of a model tailored towards static data with an RNN as its preprocessor, e.g. [6]. Based on graphical models, [19] tackles the problem from an energy-based model perspective. In all approaches, a prevalent problem are costly inferences either based on gradient-based optimization, heuristics such as beam search or Markov chain Monte Carlo. To circumvent this, learning a model for fast approximate inference is an old idea [14] which has been applied in miscellaneous settings recently [24, 12, 23, 17].

Many formulations of state-space models based on Gaussian processes exist, of which we want to not a variational technique [7]. The only drawback is that of a lack of flexibility in the design of emission models, since the restrictions of Gaussian processes are inherited.

## 2 Preliminaries

In this section we will recap the basis of our method. We will first describe the used model family, that of recurrent neural networks and then the estimator, stochastic gradient variational Bayes (SGVB).

### 2.1 Recurrent Neural Networks

Given an input sequence  $\mathbf{x} = (x_1, \dots, x_T), x_t \in \mathbb{R}^k$  we compute the output sequence of a simple RNN  $\mathbf{y} = (y_1, \dots, y_T), y_t \in \mathbb{R}^\omega$  via an intermediary hidden state layer  $\mathbf{h} = (h_1, \dots, h_T), h_t \in \mathbb{R}^\gamma$  by recursive evaluation of the following equations:

$$h_t = f_h(x_t \mathbf{W}_{\text{in}} + h_{t-1} \mathbf{W}_{\text{rec}} + \mathbf{b}_{\text{hidden}}), \quad (2)$$

$$y_t = f_y(h_t \mathbf{W}_{\text{out}} + \mathbf{b}_{\text{out}}), \quad (3)$$

The set of adaptable parameters is given by  $\theta = \{\mathbf{W}_{\text{in}}, \mathbf{W}_{\text{rec}}, \mathbf{W}_{\text{out}}, \mathbf{b}_{\text{hidden}}, \mathbf{b}_{\text{out}}\}$ .

We found it beneficial to use fast dropout in conjunction with RNNs (FD-RNNs) [1] for this work. Fast dropout is a deterministic approximation of the dropout regularization technique [16] in which

each of the network's units is described by its expectation and variance. This accounts for the output units as well, leading to an alternative of modelling the output variance as another response variable [2].

Adaptation of the network's behaviour can be done by optimizing a loss function with respect to the network's parameters with gradient-based schemes. Consider a data set of finite size, i.e.  $\mathcal{D} = \{(\mathbf{x}_{1:T}^{(i)})\}_{i=1}^I$  on which the loss operates. In a setting as in Equation (1), this will be given by  $\mathcal{L}_{\text{OSP}}(\theta) = -\sum_{i=1}^I \sum_{t=1}^T \log p(x_t | \mathbf{x}_{1:t-1})$ , which is the negative log-likelihood of the data.

## 2.2 Stochastic Gradient Variational Bayes

Stochastic gradient variational Bayes was introduced independently by [23] and [17]. For this paper, we will review the method briefly in order to introduce notation. We are interested in modelling the data distribution  $p(\mathbf{x})$  with the help of unobserved latent variable  $\mathbf{z}$  represented as a directed graphical model, i.e.  $p(\mathbf{x}) = \int p(\mathbf{x}|\mathbf{z})p(\mathbf{z})d\mathbf{z}$ . The integral is in general intractable, which is why we will use a variational upper bound on the negative log-likelihood for learning.

$$-\log p(\mathbf{x}) = -\log \int p(\mathbf{x}|\mathbf{z})p(\mathbf{z})d\mathbf{z} \quad (4)$$

$$= -\log \int \frac{q(\mathbf{z})}{q(\mathbf{z})} p(\mathbf{x}|\mathbf{z})p(\mathbf{z})d\mathbf{z} \quad (5)$$

$$\leq KL(q(\mathbf{z})|p(\mathbf{z})) - \mathbb{E}_{\mathbf{z} \sim q}[\log p(\mathbf{x}|\mathbf{z})] =: \mathcal{L}. \quad (6)$$

where  $KL(q|p)$  denotes the Kullback-Leibler divergence between two distributions  $q$  and  $p$ . Interestingly,  $q(\mathbf{z})$  can be chosen to be an arbitrary distribution. In fact, it can even be conditioned on  $\mathbf{x}$  itself, i.e. we can choose  $q(\mathbf{z}|\mathbf{x}) = f(\mathbf{x})$ . In this case, we call  $q$  the *recognition model* since it allows for fast approximate inference of the latent variables  $\mathbf{z}$  given the observed variables  $\mathbf{x}$ . The *generating model* is  $p(\mathbf{x}|\mathbf{z})$ . Note that  $q$  is a variational approximation of  $p(\mathbf{z}|\mathbf{x})$ , which cannot be found in closed form general.

Both the recognition and the generating model can be chosen arbitrarily in their computational form with the possibility to represent probability distributions as outputs and stochastic training being the only requirements. In order to minimise the upper bound of the negative log-likelihood  $\mathcal{L}$  with numerical means, it is convenient to choose multilayer perceptrons. In that case we write  $p(\mathbf{x}|\mathbf{z}, \theta^g)$  and  $q(\mathbf{z}|\mathbf{x}, \theta^r)$  to make the dependency on the respective parameter sets explicit. Learning good parameters can then be done by performing stochastic optimization of  $\mathcal{L}$  with respect to both  $\theta^r$  and  $\theta^g$ . The expectation term is then approximated by single draws from  $q$  in each training step.

Designing a model is then done by the following steps: (1) Choice of a prior  $p(\mathbf{z})$  over the latent variables. (2) Choice of recognition model  $q(\mathbf{z}|\mathbf{x}, \theta^r)$ . The Kullback-Leibler divergence between the prior and the recognition model has to be tractable and efficient to compute. (3) Choice of a generating model  $p(\mathbf{x}|\mathbf{z}, \theta^g)$ , which is mostly given by the type of data under investigation.

We want to stress that even if  $p(\mathbf{z})$  follows a distribution with a single maximum (e.g. a Gaussian) and factorises, the induced  $p(\mathbf{x})$  will generally be multi-modal. First note that to introduce dependencies between the components of  $\mathbf{x}$ , the map  $f: \mathbf{z} \mapsto \mathbf{x}$  has merely to be a rotation. For introducing new modes, an informal argument is more involved. Let  $\mathbf{x} \in \mathcal{X}$ ,  $\mathbf{z} \in \mathcal{Z}$  and  $f$  be a parametrised universal approximator (such as an MLP or an RNN). If  $f$  is smooth, arbitrary connected subsets  $X_k \subset \mathcal{X}$  will be mapped to arbitrary connected subsets  $Z \subset \mathcal{Z}$ . This allows changes in volume and hence probability density, possibly giving rise to new maxima of the probability landscape.

## 3 Methods

Extending SGVB to sequences requires an appropriate factorisation of Equation (1) along with a sensible introduction of latent variables. Further, adequate choices for the recognition model, the generating model and the prior on the latent state sequences are necessary.

The design of the recognition and generating model depend on the exact factorisation chosen. Some feedback exists as well, as the range of models available can also influence the factorisation. The

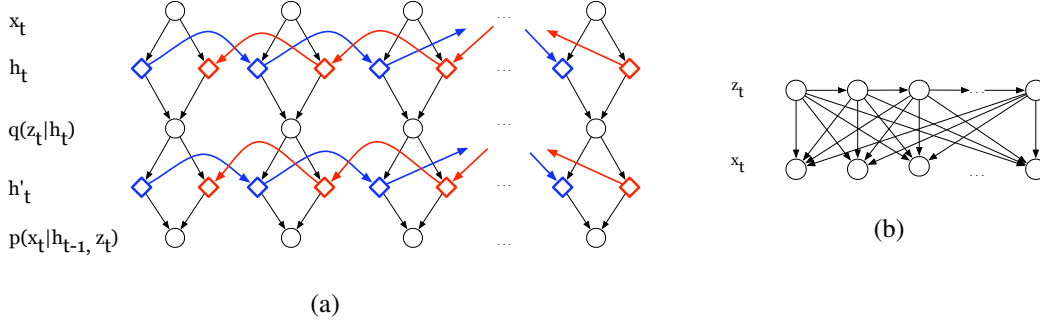


Figure 1: Illustration of (a) the computational graph and (b) the graphical model of the variational recurrent auto encoder. Diamonds are used to indicate that variables are deterministic, i.e. follow a Dirac distribution. The model uses the same deviation of the variational upper bound as the variational auto encoder [17] but additionally exploits the temporal structure of the problem. This enables the use of bidirectional recurrent networks as recognition and generating models.

generating model is required to turn samples from the prior into samples from the data generating distribution. This suggests a trade off: a richer prior which can represent many of the sequence’s aspects locally in time, will make the task of the generating model easier. Still, we need to be able to compute the KL divergence in Equation (6). As an extreme case, consider a very simple prior which factorises over time steps, e.g. independent standard Normals. In this case, the prior will only represent the “updates” and the generating model is required to keep a memory by itself. More so, the consequences of  $z_t = z_k, t \neq k$  on  $\mathbf{x}_{1:T}$  will be very different and depend on the complete sequence  $\mathbf{z}_{1:T}$ , which introduces a much tighter coupling between the different  $z_t$ . Therefore we advocate the use of priors which are as expressive as possible while still being tractable.

This section serves the introduction of two different types of latent variables in factorisations of Equation (1). We will then discuss a suitable compromise for the choice of prior.

### 3.1 Variational Recurrent Auto Encoder

Consider a model where the sequence of latent states  $\mathbf{z}_{1:T}$  is a first-order Markov chain and completely connected to each of the observed variables  $\mathbf{x}_{1:T}$ . The graphical model is depicted in Figure 1 (b).

While sampling in this model is possible via ancestral sampling, about any other inference task is hard: given a single observation  $x_t$ , all of the  $\mathbf{z}_{1:T}$  become coupled. A successful application of Markov chain Monte Carlo is doubtful due to that strong coupling.

SGVB on the other hand is a promising candidate: approximate inference of the latent states can be done efficiently, given we are using a powerful recognition model. Further, we are rather free in the choice of generating model. Yet, a rich model will take off burden from the latent state sequences and the recognition model, as argued above.

A suitable framework for mapping a sequence to another sequence of equal length is that of bidirectional recurrent neural networks [25] using fast dropout, which we employ in the generating and the recognition model. The computational graph is shown in Figure 1 (a).

This model can thus be perceived as a static variational auto encoder where both the encoder (i.e. recognition model) and the decoder (i.e. generating model) are recurrent networks and the prior  $p(\mathbf{z}_{1:T})$  has a temporal structure. The lower bound then is as follows:

$$-\log p(\mathbf{x}_{1:T}) \leq KL(q(\mathbf{z}_{1:T})|p(\mathbf{z}_{1:T})) - \mathbb{E}_{\mathbf{z}_{1:T} \sim q}[\log p(\mathbf{x}_{1:T}|\mathbf{z}_{1:T})] =: \mathcal{L}_{\text{VRAE}},$$

where we have merely added the time indices to the latent variables of Equation (6).

### 3.2 Variational One Step Predictor

A downside of the VRAE is that it is not suitable to online settings, since we need access to  $\mathbf{x}_{t+1:T}$  when we want to reason about  $x_t$ . Hence, the variational one step predictor (VOSP) is about making

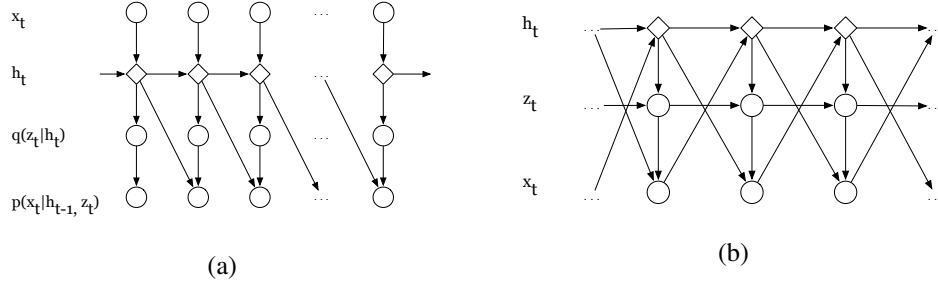


Figure 2: We show (a) the computational graph and (b) the graphical model of the variational one step predictor. In both diagrams, the dependency on the hidden states of the RNN are made explicit. Diamonds are used to show that variables are deterministic (i.e. distributed according to a Dirac). Note that the computational flow into a prediction  $p(x_t|\mathbf{x}_{1:t-1})$  from the previous hidden state  $h_{t-1}$  is entirely deterministic.

predictions using the past only. Creating a hybrid between the variational auto encoder [17] and a standard one step prediction RNN, we let the already observed past  $\mathbf{x}_{1:t-1}$  deterministically flow into the prediction of  $x_t$ .

For the computational architecture, we make use of a recurrent recognition model. To reflect the use of an RNN, we introduce additional latent variables  $h_t$  which act as a summary of the already observed sequence  $\mathbf{x}_{1:t}$  and have a Dirac distribution with infinite mass at a single point. For the generating model we use a multilayer perceptron which takes the recognition models hidden state  $h_t$  and the latent variable  $z_t$  as an input. We did not consider using an RNN as generating model. The relation between  $x_t$  and  $h_{t-1}$  is already deterministic, and introducing a dependency on  $\mathbf{z}_{1:t-1}$  would only add uncertainty.

The objective function used is then derived as follows:

$$\begin{aligned}
-\log p(\mathbf{x}_{1:T}) &= -\log \prod_{t=1}^T p(x_t|\mathbf{x}_{1:t-1}) \\
&= -\log \prod_{t=1}^T \int_{h_t} p(x_t|h_t, \mathbf{x}_{1:t-1}) dh_t \\
&= -\log \prod_{t=1}^T p(x_t|h_t),
\end{aligned}$$

where we have used the fact that  $x_t$  is conditionally independent of  $\mathbf{x}_{1:t-1}$  given  $h_t$  and  $h_t$  is following a Dirac distribution. We then introduce a set of latent variables  $\mathbf{z}_{1:T}$  which we marginalise over. Assuming that each  $x_t$  is conditionally independent of  $\mathbf{z}_{1:t-1}$  and  $\mathbf{z}_{t+1:T}$  given  $z_t$  lets us arrive at

$$-\log p(\mathbf{x}_{1:T}) = -\log \int_{\mathbf{z}_{1:T}} p(\mathbf{z}_{1:T}) \prod_{t=1}^T p(x_t|h_t, z_t) d\mathbf{z}_{1:T}.$$

We then obtain a variational upper bound by use of Jensen's inequality:

$$\begin{aligned}
-\log p(\mathbf{x}_{1:T}) &= -\log \int_{\mathbf{z}_{1:T}} \frac{q(\mathbf{z}_{1:T})}{q(\mathbf{z}_{1:T})} p(\mathbf{z}_{1:T}) \prod_{t=1}^T p(x_t|h_t, z_t) d\mathbf{z}_{1:T} \\
&\leq KL(q(\mathbf{z}_{1:T})|p(\mathbf{z}_{1:T})) - \mathbb{E}_{\mathbf{z}_{1:T} \sim q} \left[ \sum_{t=1}^T \log p(x_t|h_t, z_t) \right] \\
&=: \mathcal{L}_{\text{VOSP}}.
\end{aligned}$$

We show the graphical model and the computational graph in Figure 2.

### 3.3 Choice of Prior for $\mathbf{z}_{1:T}$

In contrast to the static case, the choice of a prior  $p(\mathbf{z}_{1:T})$  is not so obvious. Ideally, a multivariate Gaussian (MVG) is appealing since these distributions are well understood and computation of quantities of interest, e.g. the Kullback-Leibler divergence in our case, is tractable. A suitable framework for MVGs is that of Gaussian processes (GPs) [22] where the prior belief about the latent state sequence can be formulated via an appropriate Kernel function  $k$ . Let  $h_t^{(i)}$  denote the  $i$ 'th component at the  $t$ 'th time step. Then we formally write

$$h_t^{(i)} \sim GP(0, k(t, r)),$$

where the degree by which two states vary together is expressed only in terms of their respective time indices. Consequently, the latent states are jointly distributed as  $\mathbf{z}_{1:T,i} \sim \mathcal{N}(\mathbf{0}, \Sigma^z)$  with  $\Sigma_{t,r}^z = k(t, r)$ . Note that the kernel is not restricted to be stationary, which is a reasonable assumption for many data sources.

The Kullback-Leibler divergence between two MVGs  $p = \mathcal{N}(\mu_p, \Sigma_p)$  and  $q = \mathcal{N}(\mu_q, \Sigma_q)$  is given by

$$KL(q|p) = \frac{1}{2} \left[ \log \frac{|\Sigma_p|}{|\Sigma_q|} - \gamma + \text{trace}(\Sigma_p^{-1} \Sigma_q) + (\mu_p - \mu_q)^T \Sigma_p^{-1} (\mu_p - \mu_q) \right].$$

A computational issue is the quadratic runtime. Even if the necessary inverses and appropriate decompositions are precomputed, costly dot products have to be evaluated. One way to circumvent this issue is to restrict ourselves to covariance structures for which multiplication is easy. This is the case for diagonal and block-diagonal covariances, both of which regrettably are not particularly appealing for modelling time series: the implication is that distinct subsequences of a sequence are independent of each other.

Another approach is to not express our belief about the latent state sequences as  $p(\mathbf{z}_{1:T})$ , but as  $p(g(\mathbf{z}_{1:T}))$ . As long as  $g$  is linear, both distributions will maintain Gaussianity. If  $g(\mathbf{z}_{1:T})$  has a block-diagonal covariance, we can efficiently calculate the Kullback-Leibler divergence in the transformed space, i.e.  $KL(q(g(\mathbf{z}_{1:T})|\mathbf{x}_{1:T})|p(g(\mathbf{z}_{1:T})))$ .

This framework lets us use a Wiener process as a prior on the latent state sequences. If we are using the map

$$g_W(\mathbf{z}_{1:T}) = (z_0, z_1 - z_0, z_2 - z_1, \dots, z_T - z_{T-1})$$

with  $p(g_W(z_t)) \sim \mathcal{N}(0, 1)$ , we will obtain a Wiener process, i.e.  $z_t^{(i)} \sim \mathcal{GP}(0, \min(r, t))$ . In practice, we will obtain a prediction from the recognition model, i.e.  $q(\mathbf{z}_{1:T}|\mathbf{x}_{1:T})$  which is a Gaussian with diagonal covariance. Transforming that Gaussian with  $g_W$  and obtaining the KL divergence from a white Gaussian will then correspond to direct calculation of the KL divergence from a Wiener process.

## 4 Experiments on Musical Data

The musical data consist of three<sup>2</sup> distinct data sets of piano rolls named ‘‘JSBChorales’’, ‘‘Piano-midi.de’’, and ‘‘Nottingham’’. At each time step, a binary variable is given for 88 different tones, each of which indicates whether that tone is present at that moment. The high dimensionality and the complex interdependencies of notes at a single time step make it an ideal test bed for the evaluation of models that are designed to excel in this situation.

We design a single component of the posterior over observed variables given the latent variables  $p(\mathbf{x}_{1:T}|\mathbf{z}_{1:T})$  in the case of VRAE and  $p(x_t|h_{t-1}, z_t)$  to be distributed according to independent Bernoulli distributions. For priors, we use as Wiener process as described in Section 3.3.

The same split into training, validation and test sets as done in the previous publications relying on that benchmark [20, 3, 1] was used.

<sup>2</sup>Experiments on the fourth data set, ‘‘MuseData’’ did not complete at the time of submission of this article.

#### 4.1 Learning the model parameters

Learning constitutes to the minimisation of the variational upper bounds  $\mathcal{L}_{\text{VRAE}}$  and  $\mathcal{L}_{\text{VOSP}}$ . To evaluate the performance of the proposed methods we conducted a random search over the possible hyper parameters, using 64 samples for each data set; more details on the learning are given in the supplementary material.

We report the loss of the model on the unsplit testing sequences for which the loss on the splitted validation sequences was lowest. Note that the loss is an upper bound of the negative log-likelihood, in contrast to the results from the other models for which we report the negative log-likelihood.

The VRAE model achieves state-of-the-art performance in two of the three data sets. VOSP does not supprass RNN-Nade, but is still obtaining a significant edge over the one step prediction based RNNs. We give the results in table 1.

#### 4.2 Online Denoising

For a demonstration of denoising we selected the VOSP model and parameters best performing on the “Nottingham” data set. Note that this denoising process is thus purely online, i.e. it only requires data from the past to denoise the present.

In denoising, one is usually interested in the most likely true data  $\hat{\mathbf{x}}$  giving rise to observed data  $\mathbf{x}$ . A proper probabilistic treatment would then be to select the most likely  $\tilde{\mathbf{x}}$  given the observation  $\mathbf{x}$  while marginalizing over the latent states  $\mathbf{z}$ , i.e.  $\hat{\mathbf{x}} = \text{argmax}_{\tilde{\mathbf{x}}} \int_{\mathbf{z}} p(\tilde{\mathbf{x}}|\mathbf{z})p(\mathbf{z}|\mathbf{x})d\mathbf{z}$ . To avoid costly operations, we perform two approximations for our denoising method: (a) we find a maximum likelihood estimation of  $\mathbf{z}$  and (b) we do so using the approximation  $q$  instead of the true posterior, i.e.

$$\begin{aligned}\tilde{\mathbf{z}} &= \text{argmax}_{\mathbf{z}} q(\mathbf{z}|\mathbf{x}), \\ \tilde{\mathbf{x}} &= \text{argmax}_{\mathbf{x}} p(\mathbf{x}|\tilde{\mathbf{z}}).\end{aligned}$$

Qualitative results are shown in Figure 3.

#### 4.3 Missing value imputation

For missing value imputation we selected the best VRAE model and parameters from the “Nottingham” data set as well. We followed a procedure similar to that described by [23]. First, the missing values of  $\mathbf{x}_{1:T}$  are set to random values between 0 and 1. Then, the following actions are looped over for a fixed number of steps:

1. Select the mode of the recognition model’s approximate posterior  $\hat{\mathbf{z}}_{1:T} = \text{argmax}_{\mathbf{z}_{1:T}} q(\mathbf{z}_{1:T}|\mathbf{x}_{1:T})$ ,
2. Select the mode of the posterior over the visibles  $\hat{\mathbf{x}}_{1:T} = \text{argmax}_{\mathbf{x}_{1:T}} p(\mathbf{x}_{1:T}|\hat{\mathbf{z}}_{1:T})$ ,
3. Update the missing elements of  $\mathbf{x}$  with those from  $\hat{\mathbf{x}}$ ,

This method does not sample from the conditional of the missing values given the observed ones, but we found it to be an effective and fast method to obtain a point estimate. We show qualitative results in Figure3.

### 5 Conclusion

We have presented two different ways of introducing latent variables into time series models. Based on neural networks as the central building blocks and thanks to recent advances in variational learning of directed graphical models, we were able to succesfully train them on well established benchmarks. The results obtained place our method among the state of the art. The experiments further confirmed our hypothesis that these models exhibit high performance in structured output settings; this is illustrated by the huge advantage in performance between to the models which treat the outputs as conditionally independent. We further verified the quality of the obtained solutions in the highly practical data processing tasks of missing value imputation and online denoising.

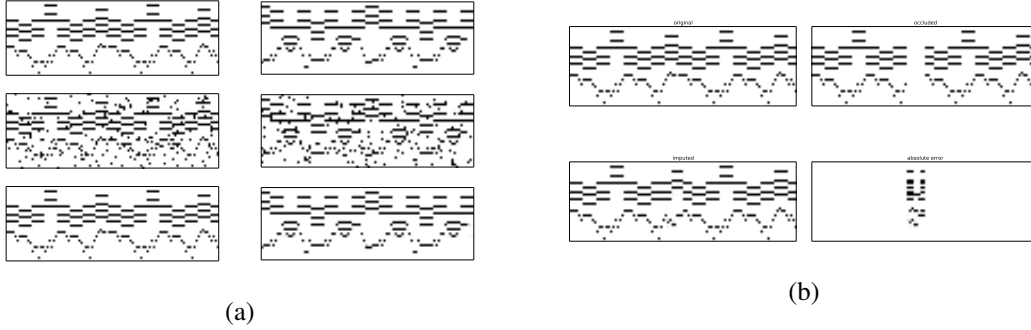


Figure 3: Visualizations of (a) denoising and (b) missing value imputation. *Denoising*: we show two different sequences corresponding to the columns. The first row is the clean data. Each note was turned on with a probability of 0.05. The bottom row shows the denoised song. *Missing value imputation*: We corrupted a single song by removing complete information over a period of eight time steps. Top left: original. Top right: corrupted. Bottom left: recovered. Bottom right: errors.

Table 1: Results on the midi data sets. All numbers except ours are average negative log-likelihoods on the test set. In our case, an upper bound on the negative log-likelihood is obtained. “FD” represents the work of [1]; “plain” and “RNN-NADE” results are from [3] while “Deep RNN” shows the best results from [20]. Only “VRAE”, “VOSP” and “RNN-NADE” do not treat the different components of  $x_t$  as conditionally independent given the past  $\mathbf{x}_{1:t-1}$ . This is a possible explanation for the huge gap between them and the other models, which have an array of logistic regression models as their final output layer.

Data set	VRAE	VOSP	FD	plain	RNN-NADE	Deep RNN
Piano-midi.de	< 4.00	< 6.08	7.39	7.58	7.05	—
Nottingham	< 2.00	< 2.63	3.09	3.43	2.31	2.95
JSBChorales	< 5.53	< 6.21	8.01	8.58	5.19	7.92



## 6 Acknowledgements

We thank Durk Kingma and Maximillian Karl for valuable discussions. This work bases heavily on Theano [?].

## References

- [1] Justin Bayer, Christian Osendorfer, Daniela Korhammer, Nutan Chen, Sebastian Urban, and Patrick van der Smagt. On fast dropout and its applicability to recurrent networks. *arXiv preprint arXiv:1311.0701*, 2013.
- [2] Justin Bayer, Christian Osendorfer, Sebastian Urban, et al. Training neural networks with implicit variance. In *Proceedings of the 20th International Conference on Neural Information Processing, ICONIP-2013*, 2013.
- [3] Y. Bengio, N. Boulanger-Lewandowski, and R. Pascanu. Advances in optimizing recurrent networks. *arXiv preprint arXiv:1212.0901*, 2012.
- [4] Yoshua Bengio and Éric Thibodeau-Laufer. Deep generative stochastic networks trainable by backprop. *arXiv preprint arXiv:1306.1091*, 2013.
- [5] Christopher M Bishop. Mixture density networks. 1994.
- [6] Nicolas Boulanger-Lewandowski, Yoshua Bengio, and Pascal Vincent. High-dimensional sequence transduction. In *ICASSP*, 2013.
- [7] Andreas C Damianou, Michalis K Titsias, and Neil D Lawrence. Variational gaussian process dynamical systems. In *NIPS*, pages 2510–2518, 2011.
- [8] Alex Graves. Practical variational inference for neural networks. In *Advances in Neural Information Processing Systems*, pages 2348–2356, 2011.
- [9] Alex Graves. Generating sequences with recurrent neural networks. *arXiv preprint arXiv:1308.0850*, 2013.
- [10] Alex Graves, Santiago Fernández, Marcus Liwicki, Horst Bunke, and Jurgen Schmidhuber. Unconstrained online handwriting recognition with recurrent neural networks. *Advances in Neural Information Processing Systems*, 20:1–8, 2008.
- [11] Alex Graves, Abdel-rahman Mohamed, and Geoffrey Hinton. Speech recognition with deep recurrent neural networks. *arXiv preprint arXiv:1303.5778*, 2013.
- [12] Karol Gregor and Yann LeCun. Learning fast approximations of sparse coding. In *Proceedings of the 27th International Conference on Machine Learning (ICML-10)*, pages 399–406, 2010.
- [13] Michiel Hermans and Benjamin Schrauwen. Training and analysing deep recurrent neural networks. In *Advances in Neural Information Processing Systems*, pages 190–198, 2013.
- [14] Geoffrey E Hinton, Peter Dayan, Brendan J Frey, and Radford M Neal. The” wake-sleep” algorithm for unsupervised neural networks. *SCIENCE-NEW YORK THEN WASHINGTON-*, pages 1158–1158, 1995.
- [15] Geoffrey E Hinton, Simon Osindero, and Yee-Whye Teh. A fast learning algorithm for deep belief nets. *Neural computation*, 18(7):1527–1554, 2006.
- [16] Geoffrey E Hinton, Nitish Srivastava, Alex Krizhevsky, Ilya Sutskever, and Ruslan R Salakhutdinov. Improving neural networks by preventing co-adaptation of feature detectors. *arXiv preprint arXiv:1207.0580*, 2012.
- [17] Diederik P Kingma and Max Welling. Auto-encoding variational bayes. *arXiv preprint arXiv:1312.6114*, 2013.
- [18] Tomas Mikolov, Martin Karafiát, Lukáš Burget, Jan Cernocky, and Sanjeev Khudanpur. Recurrent neural network based language model. *Proceedings of Interspeech*, 2010.
- [19] Piotr Mirowski and Yann LeCun. Dynamic factor graphs for time series modeling. In *Machine Learning and Knowledge Discovery in Databases*, pages 128–143. Springer, 2009.
- [20] Razvan Pascanu, Caglar Gulcehre, Kyunghyun Cho, and Yoshua Bengio. How to construct deep recurrent neural networks. *arXiv preprint arXiv:1312.6026*, 2013.
- [21] Razvan Pascanu, Tomas Mikolov, and Yoshua Bengio. On the difficulty of training recurrent neural networks. Technical report, Technical Report, 2012.
- [22] Carl Edward Rasmussen. *Gaussian processes for machine learning*. Citeseer, 2006.
- [23] Danilo Jimenez Rezende, Shakir Mohamed, and Daan Wierstra. Stochastic back-propagation and variational inference in deep latent gaussian models. *arXiv preprint arXiv:1401.4082*, 2014.

- [24] Stephane Ross, Daniel Munoz, Martial Hebert, and J Andrew Bagnell. Learning message-passing inference machines for structured prediction. In *Computer Vision and Pattern Recognition (CVPR), 2011 IEEE Conference on*, pages 2737–2744. IEEE, 2011.
  
- [25] Mike Schuster. Better Generative Models for Sequential Data Problems: Bidirectional Recurrent Mixture Density Networks. In *Neural Information Processing Systems*, pages 589–595, 1999.
  
- [26] I. Sutskever. *Training Recurrent Neural Networks*. PhD thesis, University of Toronto, 2013.
  
- [27] Ilya Sutskever, James Martens, George Dahl, and Geoffrey Hinton. On the importance of initialization and momentum in deep learning. 2013.
  
- [28] T. Tieleman and G.E. Hinton. Lecture 6.5 - rmsprop: Divide the gradient by a running average of its recent magnitude. COURSERA: Neural Networks for Machine Learning, 2012.
  
- [29] Sida Wang and Christopher Manning. Fast dropout training. In *Proceedings of the 30th International Conference on Machine Learning (ICML-13)*, pages 118–126, 2013.

## Appendix

### FD RNNs

We will provide a short review, but urge the reader to consult [1, 29] for more details.

The following calculation of the hidden state and the output sequence are used.

$$\begin{aligned}
E[a_t] &= d_x E[\mathbf{x}_t] \mathbf{W}_{\text{in}} + d_h E[\mathbf{h}]_{t-1} \mathbf{W}_{\text{rec}} \\
V[a_t] &= ((1 - d_x) d_x E[\mathbf{x}_t]^2 + d_x V[\mathbf{x}_t] \mathbf{W}_{\text{in}}^2 + ((1 - d_h) d_h E[\mathbf{h}_{t-1}]^2 + d_h V[\mathbf{h}]_{t-1} \mathbf{W}_{\text{rec}}^2 \\
E[h_t] &= f_h^E(E[a_t], V[a_t]) \\
V[h_t] &= f_h^V(E[a_t], V[a_t]) \\
E[v_t] &= d_o E[h_t] \mathbf{W}_{\text{out}} \\
V[v_t] &= ((1 - d_o) d_o E[h_t]^2 + d_o V[h_t] \mathbf{W}_{\text{out}}^2 \\
E[y_t] &= f_y^E(E[v_t], V[v_t]) \\
V[y_t] &= f_y^V(E[v_t], V[v_t])
\end{aligned}$$

The complementary dropout rates are given by  $d_x, d_h, d_o$ . The *pre synaptic* activations of a hidden unit, i.e. before the application of a non linear transfer function are given by  $a_t$ . The *post synaptic* values are referred to as  $h_t$ . Likewise,  $v_t$  and  $y_t$  correspond to the pre and post synaptic moments of the output. The application of the transfer functions themselves  $f_h$  and  $f_y$  require special transfer functions  $f_h^E, f_h^V, f_y^E, f_y^V$  which solve the integrals  $f^E(a) = \int f(x) \mathcal{N}(x|E[a], V[a]) dx$  and  $f^V(a) = \int (f(x) - f^E(x))^2 \mathcal{N}(x|E[a], V[a]) dx$ .

### Details on Learning

Since overfitting is naturally dealt with by the variational lower bound, we can release the fixed dropout rates of the recognition models and instead integrate them into the set of adaptable parameters  $\theta$ , obtaining an effect of learned noise injection instead of regularizers.

The runtime was decreased by organising sequences into chunks of length 100. Sequences shorter than that were prepadded with zeros during the forward propagation, but the corresponding terms of the loss were set to zero to remove any bias.

For optimization, we used *rmsprop* [28], an optimizer which divides the gradient by an exponential moving average of its squares. We found that enhancing *rmsprop* with Nesterov's accelerated gradient [26] greatly reduces the training time in preliminary experiments.

To initialize the RNNs to stable dynamics we followed the initialization protocol of [27] of setting the spectral radius  $\rho$  to a specific value and the maximum amount of incoming connections of a unit to  $\nu$ ; we did not find it necessary to centre the inputs and outputs. The effect of not only using the recurrent weight matrix for propagating the states through time but also its element-wise square for advancing the variances can be quantified. We also use the gradient clipping method introduced in [21], with a fixed threshold of 225. We used drop out rates of 0.1 if not specified otherwise.

### Hyper parameters

We show the hyper parameters ranges for in Table 2.

Table 2: Hyper parameter ranges and parameter distributions for the musical data sets.

Hyper parameter	Choices
#hidden layers	1
#hidden units	200, 400, 600
Transfer function	tanh
Step rate	0.01, 0.005, 0.001, 0.0005, 0.0001, 0.00001
Momentum	0.0, 0.9, 0.95, 0.99, 0.995
Decay	0.8, 0.9
$\mathbf{W}_{\text{rec}}$	$\mathcal{N}(0, \sigma^2), \sigma^2 \in \{0.1, 0.01, 0.001, 0.0001\}$
$\mathbf{W}_{\text{in}}$	$\mathcal{N}(0, \sigma^2), \sigma^2 \in \{0.1, 0.01, 0.001, 0.0001\}$
$b_h$	<b>0</b>
$b_y$	<b>-0.8</b>
$\rho(\mathbf{W}_{\text{rec}})$	1.0, 1.05, 1.1, 1.2
$\nu$	15, 25, 35, 50 or no